JOURNAL OF MATERIALS SCIENCE 26 (1991) 6091–6096

Observations and analyses of microstructural defects for chemical vapour deposited β-SiC by transmission electron microscopy

YANG-MING LU, MIN-HSIUNG HON
Department of Materials Engineering, National Cheng Kung University, Tainan, Taiwan
WHAI-YUH LIN
Materials Research and Development Centre, Chung Shan Institute of Science and Technology, Taiwan

A transparent silicon carbide was grown by a cold-wall chemical vapour deposition (CVD) system using CH_3SiCl_3 and hydrogen gas mixtures on to a graphite substrate. Transmission electron microscopy was used to observe microstructural defects of CVD β-SiC, using $\boldsymbol{g}.\boldsymbol{b} = 0, \pm 1/3$ and the $\boldsymbol{g}.\boldsymbol{R}_F$ = integer criterion, quantitative information on defects can be obtained. The $\boldsymbol{b}$ was identified as 1/6 [1 1 $\bar{2}$] for Shockley partial dislocations and $\boldsymbol{R}_F$ as 1/3 [$\bar{1}$ 1 1], 1/3 [1 $\bar{1}$ 1], 1/3 [1 1 $\bar{1}$] for stacking faults. Twin planes were identified as (1 1 $\bar{1}$), ($\bar{1}$ 1 $\bar{1}$) in this study. Stacking faults and twins always existed on {1 1 1}. Subgrains were surrounded by dislocation networks and full of microtwins. Other defects, such as dislocation loops and dislocation dipoles, were also observed.

1. Introduction

It is well known that many kinds of defect exist in chemical vapour deposited (CVD) SiC, such as stacking faults, twins, dislocations, dislocation loops, dislocation dipoles, etc. [1, 2]. When a crystal lattice is conceived in terms of the stacking of layers in a well-defined manner, any error in the regular sequence of the layers is known as a stacking "fault", "mistake", or "disorder". Stacking faults may arise in the growth of crystals with well-developed layer structure, for example, silicon carbide [3], graphite [3], mica [4], and others. In this work, contrast experiments were used in which the Burgers vector of a dislocation line and the displacement vectors of stacking faults can be determined using an invisibility criteria. β-SiC with a cubic zinc blend structure [5] can be simply considered to have face centred cubic structure with silicon atoms at corner and face sites and carbon atoms at tetrahedral interstitials. With this modification, a simpler analysis could be made in which only two types of partial dislocation need to be considered for stacking faults on {1 1 1} [6], the Shockley partial with $\boldsymbol{b} = \langle 1\,1\,2 \rangle$ and the Frenk partials with $\boldsymbol{b} = \langle 1\,1\,1 \rangle$. The partial dislocation will be effectively invisible if $\boldsymbol{g}.\boldsymbol{b}$ is zero or $\pm 1/3$, but visible for other values of $\boldsymbol{g}.\boldsymbol{b}$. If $\boldsymbol{R}_F$, is defined as the displacement of the crystal below the planar defect with respect to the top of the crystal, $2\pi \boldsymbol{g}.\boldsymbol{R}_F = 0$ or an integral number of 2π, no displacement fringes will be visible. Diffraction patterns from twins in cubic crystal structures have been discussed in detail by a number of workers [7, 8]. A twin is simply one part of a crystal that is oriented with respect to another according to the symmetry rule. Extra spots arise in the selected-area diffraction pattern because the twin in the thin foil is oriented differently from the matrix relative to the incoming electron beam. Because the β-SiC has a cubic structure, the twin axis is parallel to the twin plane normal, thus twin planes can be determined from the diffraction patterns.

2. Experimental procedure

β-SiC was obtained from thermal decomposition of CH_3SiCl_3 with hydrogen as carrier gas in a cold-wall CVD system. The deposits were obtained by burning out graphite substrates at 800 °C in air. Then the deposits were taped on bulk metals, ground on both sides with diamond pasters until the thickness was less than 100 μm. Next, a dimple grinder was used to thin the specimens further down to 20 μm. Finally, an ion-beam thinner was used to thin the specimen for TEM observations. Table I lists the possible conditions of $\boldsymbol{g}.\boldsymbol{b}_{\text{partial}}$. Open circles represented the visible condition. Table II gives the visible and invisible conditions of stacking faults.

3. Results and discussion

From the diffraction patterns shown in Fig. 1, all the crystals investigated had the face centred cubic structure with lattice constant $a = 0.435\,98$ nm which was consistent with β-SiC. Thus considering the β-SiC

0022–2461/91 $03.00 + .12

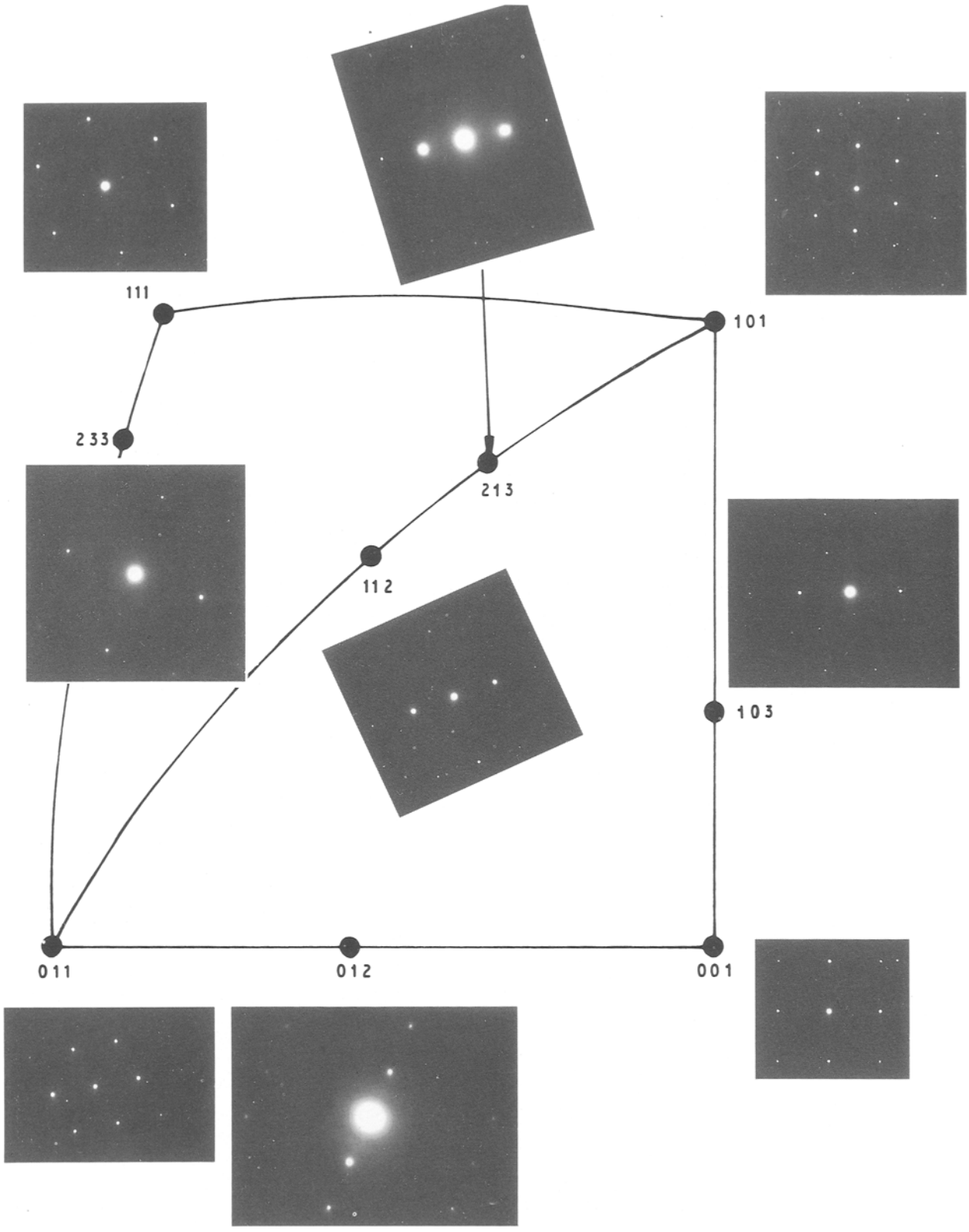

Figure 1 Low-index zones on two standard triangles: [0 1 1]–[0 0 1]–[1 0 1], [0 1 1]–[1 1 1]–[1 0 1] of CVD β-SiC.

structure to be face centred cubic close packing structure was reasonable. Fig. 2 shows images taken by the double beam method. In Fig. 2a, $\boldsymbol{g} = [\bar{1}\,1\,1]$, a partial dislocation, E, is visible, as are stacking faults A and B. In Fig. 2b, $\boldsymbol{g} = [1\,\bar{3}\,1]$, stacking fault A disappears but B is still visible. This indicates that the displacement vector, $\boldsymbol{R}_F$ of stacking faults A and B, must be different. Partial dislocations, E, and dislocation loop, L, are visible in this figure. In Fig. 2c, stacking faults B are invisible but partial dislocations E and stacking fault A are visible. In Fig. 2d, A and E have very light residual contrasts but B is clearer. For the invisible defects, images sometimes have residual contrast, so A and E are thought to be invisible. In Fig 2e, another set of stacking faults C, appear while A disappears. B becomes broader due to tilting of the specimen. In

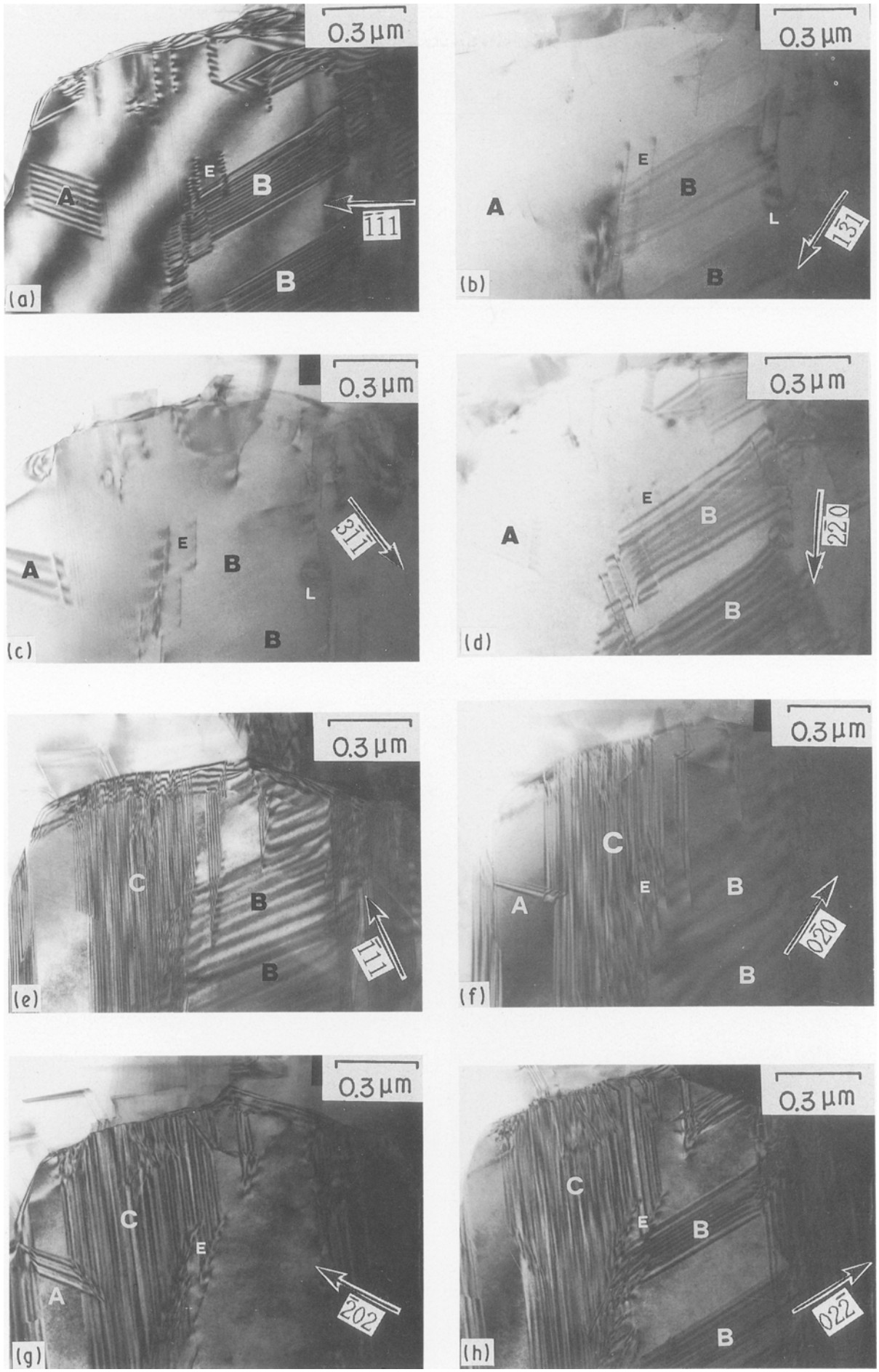

Figure 2 A ***g.b*** analysis of partial dislocation and stacking fault. The text describes the identification of 1/6 $[1\,1\,\bar{2}]$ Shockley partial dislocations, E, stacking fault displacement vectors $\boldsymbol{R}_F$: 1/3 $[\bar{1}\,1\,1]$, 1/3 $[1\,\bar{1}\,1]$, 1/3 $[1\,1\,\bar{1}]$ for A, B and C, respectively. (a) $\boldsymbol{g} = \bar{1}\,\bar{1}\,1$, (b) $\boldsymbol{g} = 1\,\bar{3}\,1$, (c) $\boldsymbol{g} = 3\,\bar{1}\,\bar{1}$, (d) $\boldsymbol{g} = 2\,\bar{2}\,0$, (e) $\boldsymbol{g} = \bar{1}\,1\,1$, (f) $\boldsymbol{g} = 0\,\bar{2}\,0$, (g) $\boldsymbol{g} = \bar{2}\,0\,2$, (h) $\boldsymbol{g} = 0\,2\,\bar{2}$.

TABLE I. The values of $\boldsymbol{g}.\boldsymbol{b}$ used to identify Burgers vector of partial dislocations. (×) $\boldsymbol{g}.\boldsymbol{b} = 0, \pm 1/3$, invisible; (○) $\boldsymbol{g}.\boldsymbol{b} \neq 0, \pm 1/3$, visible

	$\boldsymbol{b}$											
$\boldsymbol{g}$	$\frac{1}{6}[1\,1\,2]$	$\frac{1}{6}[1\,1\,\bar{2}]$	$\frac{1}{6}[1\,\bar{2}\,1]$	$\frac{1}{6}[2\,\bar{1}\,1]$	$\frac{1}{6}[\bar{1}\,1\,2]$	$\frac{1}{6}[1\,\bar{1}\,2]$	$\frac{1}{6}[1\,2\,1]$	$\frac{1}{6}[\bar{1}\,2\,1]$	$\frac{1}{6}[1\,2\,\bar{1}]$	$\frac{1}{6}[2\,1\,1]$	$\frac{1}{6}[\bar{2}\,1\,1]$	$\frac{1}{6}[2\,1\,\bar{1}]$
$\bar{1}\bar{1}1$	×	○	○	×	×	×	×	×	○	×	×	○
$1\bar{3}1$	×	○	○	○	×	○	○	○	○	×	○	×
$3\bar{1}\bar{1}$	×	○	○	○	○	×	×	○	×	○	○	○
$2\bar{2}0$	×	×	○	○	○	○	×	○	×	×	○	×
$\bar{1}11$	×	×	×	×	○	×	×	○	×	×	○	×
$0\bar{2}0$	×	×	○	×	×	×	○	○	○	×	×	×
020	×	×	○	×	×	×	○	○	○	×	×	×
$\bar{2}02$	×	○	×	×	○	×	×	○	○	×	○	○
$02\bar{2}$	×	○	○	○	×	○	×	×	×	×	×	○

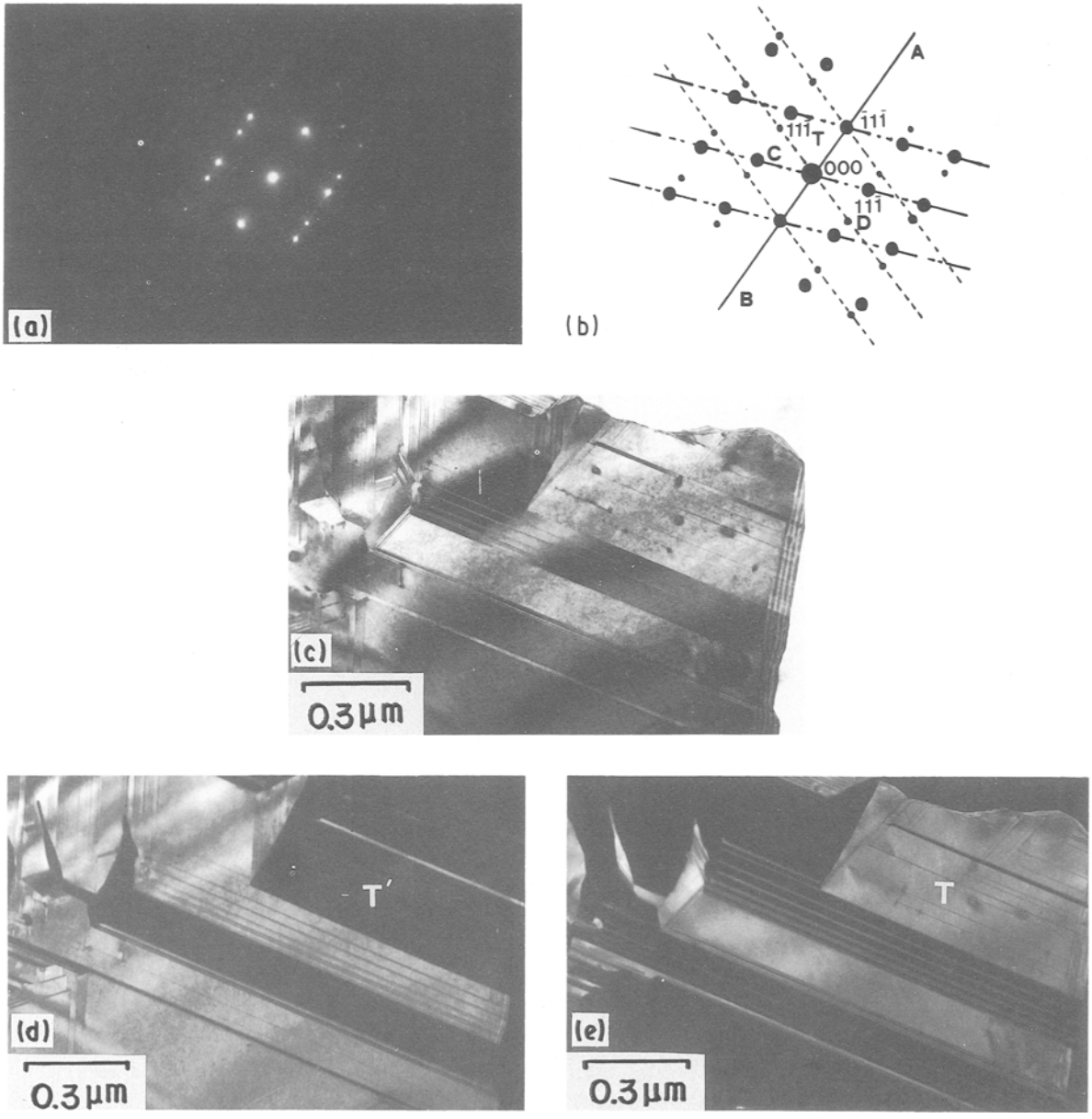

Figure 3 (1 1 1) [0 1 1] twins of β-SiC. (a) Selected-area diffraction pattern, (b) analysis of selected-area diffraction pattern, (c) bright-field images, (d) dark-field images of matrix spot C, (e) dark-field images of twin spot D.

Fig. 2f, stacking faults A, B and C are all visible. Partial dislocations E are overlapped by stacking faults C, thus some disturbances occur at the end of C. In Fig. 2g, only B is invisible, whereas in Fig. 2h, only A disappears.

From the above results, the dislocation marked E is identified as 1/6 [1 1 $\bar{2}$] Shockley partials, which is one end of stacking fault C. Thus, it can be concluded that three sets of stacking fault exist in CVD β-SiC and always occur on the {1 1 1} close packing plane.

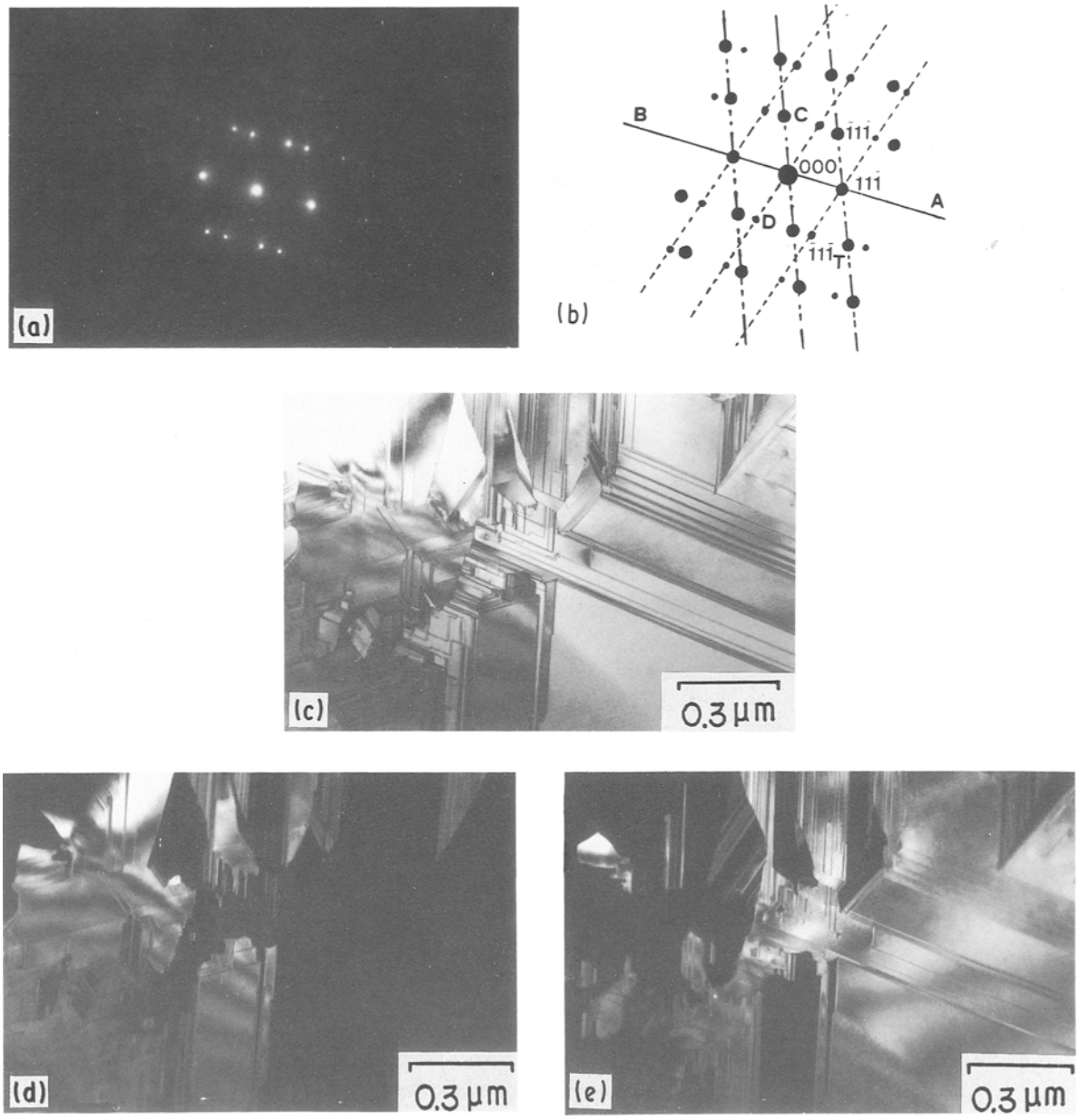

Figure 4 (1 1 $\bar{1}$) [0 1 1] twins of β-SiC. (a) Selected-area diffraction pattern, (b) analysis of selected-area diffraction pattern, (c) bright-field image, (d) dark-field image of matrix spot C, (e) dark-field image of twin spot D.

The twins of CVD β-SiC are always observed in the ⟨1 1 0⟩ zone, as shown in Figs 3 and 4. Fig. 3a is a diffraction pattern of the [0 1 1] zone in which matrix spots are accompanied by twin spot and symmetry to the twin axis $\overline{AB}$. From Fig. 3b, the twin axis $\overline{AB}$ is identified as [$\bar{1}$ 1 $\bar{1}$]. With cubic structure, the twin axis of β-SiC must be normal to the twin plane which was identified as ($\bar{1}$ 1 $\bar{1}$). Fig. 3c is a bright-field image of a twin at the exact zone with several sets of twin bands in it. Fig 3d and e are imaged by a matrix diffraction of spot C and a twin spot D, respectively. The dark part, T', in Fig. 3d becomes light, T, in Fig 3e, which confirms that the extra spots are twin spots.

A similar analysis, can be applied to Fig. 4a–e, except the twin axis $\overline{AB}$ becomes [1 1 $\bar{1}$]. Although only two twin axes have been deduced in the ⟨$\bar{1}$ 1 0⟩ zone, we believed that [$\bar{1}$ 1 1] must be another twin axis. [$\bar{1}$ 1 1] does not appear because ⟨1 1 0⟩ can show only two twin axes. Thus it is concluded that the twin planes of β-SiC are {1 1 1}. Dislocation tangles resulting from internal stresses generated during deposition are observed in some of the grains of polycrystalline CVD SiC. The micrograph shown in

TABLE II The values of $\boldsymbol{g}.\boldsymbol{R}_F$ used to identify displacement vector of stacking faults. (×) $\boldsymbol{g}.\boldsymbol{R}_F$ = integer invisible (○) $\boldsymbol{g}.\boldsymbol{R}_F \neq$ integer, visible

	$\boldsymbol{R}_F$			
$\boldsymbol{g}$	$\frac{1}{3}$[1 1 1]	$\frac{1}{3}$[$\bar{1}$ 1 1]	$\frac{1}{3}$[1 $\bar{1}$ 1]	$\frac{1}{3}$[1 1 $\bar{1}$]
$\bar{1}\bar{1}$1	○	○	○	×
1 $\bar{3}$ 1	○	×	○	×
3 $\bar{1}$ $\bar{1}$	○	○	×	×
2 $\bar{2}$ 0	×	×	○	×
$\bar{1}$ 1 1	○	×	○	○
0 $\bar{2}$ 0	○	○	○	○
0 2 0	○	○	○	○
$\bar{2}$ 0 2	×	○	×	○
0 2 $\bar{2}$	×	×	○	○

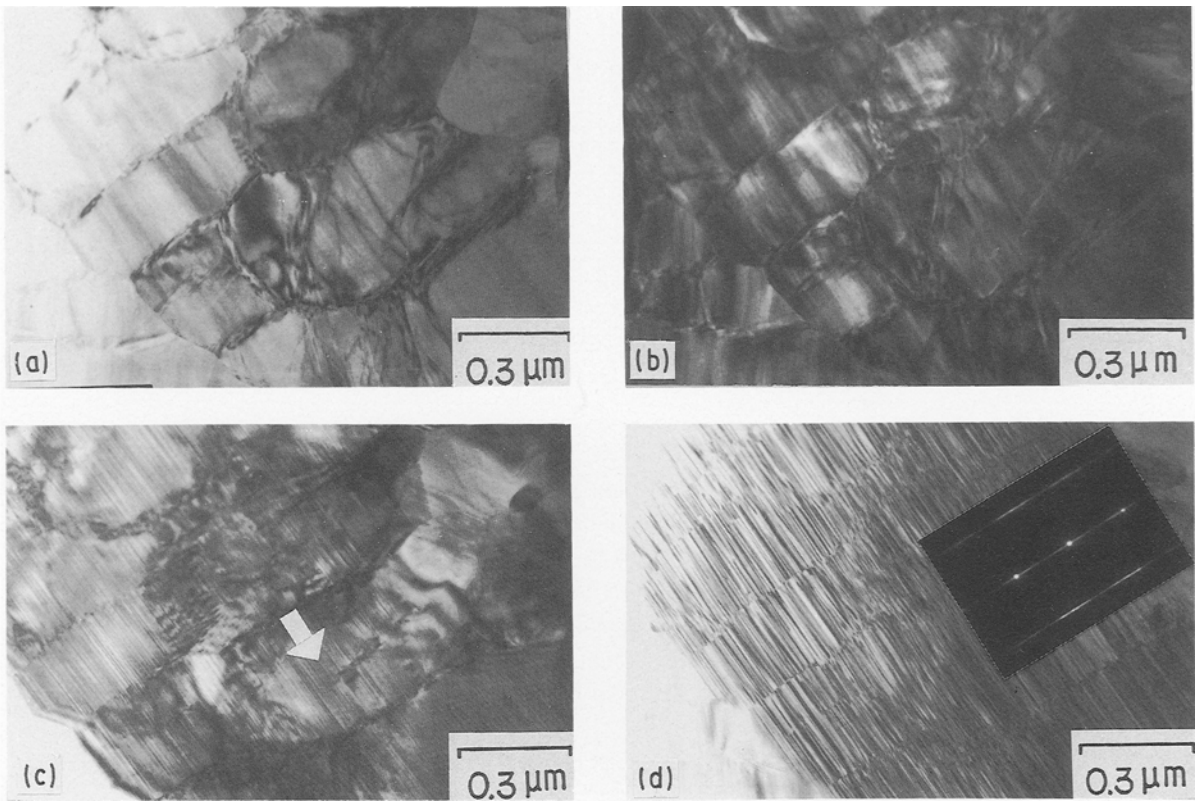

Figure 5 Tilted transmission electron micrographs of chemical vapour deposited β-SiC. (a) Dislocation tangles in the film, (b) tilted micrograph, (c) tilted micrograph, trace of microtwins can be observed (white arrow), (d) the mosaic of slightly misoriented subgrains (see inset diffraction pattern) consisting of high-density microtwins.

Figure 6 Several dislocation dipoles exist in CVD β-SiC (arrowed).

Fig. 5a indicates that the dislocations bounding the subgrains are mosaic with very small misorientations. Fig. 5b–d are tilted figures of Fig. 5a. Fig. 5d shows each subgrain is composed of stacks of $\{1\,1\,1\}$ microtwins. Ogbuji *et al.* [9] pointed out that the traces as shown in Fig. 5c are base plane traces (arrowed), but it is our opinion that they are just microtwins traces due to the tilt. Closely spaced dislocation dipoles are observed in this study as shown in Fig. 6, where the spacing of the images changes on reversing $\boldsymbol{g}$.

4. Conclusion

The stacking faults of CVD β-SiC are always on the $\{1\,1\,1\}$ close packing planes, as are twins and microtwins. The partial dislocations are identified as Shockley partials with $\boldsymbol{b} = [1\,1\,\bar{2}]$ in this study. Dislocation tangles resulting from internal stress produced during deposition form subgrain boundaries which are composed of high-density microtwins lying on $\{1\,1\,1\}$. Dislocation dipoles and dislocation loops were also found in this work.

Acknowledgements

This study was supported by National Science Council (no. NSC 79-0405-E006-37), Taiwan.

References

1. S. S. SAMUEL and H. SATO, *J. Amer. Ceram. Soc.* **61** (1978) 425.
2. L. I. VAN TONE, *J. Appl. Phys.* **37** (1965) 1849.
3. H. JAGODZINSKI, *Acta Crystallogr.* **2** (1949) 298.
4. S. B. HENDRICKS, *Phys. Rev.* **57** (1940) 448.
5. R. W. DAVIDGE, in "Mechanical Behaviour of Ceramics", edited by R. W. Cahn, M. W. Thompson and I. M. Wood, (Cambridge University Press, New York, 1979) p. 5.
6. M. H. LORETTO and R. E. SMALLMAN, in "Defect Analysis in Electron Microscopy" (Halsted Press, Wiley, New York, 1975) p. 75.
7. O. JOHARI and G. THOMAS, *Trans. AIME* **230** (1964) 597.
8. C. M. WAYMAN and R. BULLOUGH, *ibid.* **236** (1966) 1711.
9. L. U. OGBUJI, T. E. MITCHELL, A. H. HEUER and S. SHINOZAKI, *J. Amer. Ceram. Soc.* **64** (1981) 100.

Received 13 July 1990
and accepted 6 February 1991